Downloaded from rsta.royalsocietypublishing.org

PHILOSOPHICAL TRANSACTIONS OF THE ROYAL SOCIETY A MATHEMATICAL, PHYSICAL & ENGINEERING SCIENCES

Hydroelasticity of Non-Beamlike Ships in Waves [and Discussion]

A. J. Keane, P. Temarel, Xiong-Jian Wu, Yongshu Wu, D. W. Chalmers, A. J. Keane, K. Nicholson, A. Incecik, S. Hylarides and W. Beukelman

Phil. Trans. R. Soc. Lond. A 1991 **334**, 339-355
doi: 10.1098/rsta.1991.0018

Email alerting service

Receive free email alerts when new articles cite this article - sign up in the box at the top right-hand corner of the article or click **here**

To subscribe to *Phil. Trans. R. Soc. Lond. A* go to:
http://rsta.royalsocietypublishing.org/subscriptions

This journal is © 1991 The Royal Society

Downloaded from rsta.royalsocietypublishing.org

Hydroelasticity of non-beamlike ships in waves

By A. J. Keane[1], P. Temarel[2], Xiong-Jian Wu[2,4] and Yongshu Wu[3,5]

[1] *Oxford University, Parks Road, Oxford OX1 3PJ, U.K.*
[2] *Brunel University, Uxbridge, Middlesex UB8 3PH. U.K.*
[3] *Liverpool University, Liverpool L69 3BX, U.K.*
[4] *Shanghai Jiao-Tong University, Shanghai, People's Republic of China*
[5] *China Ship Scientific Research Centre, Wuxi, People's Republic of China*

[Plate 1]

The theoretical background of hydroelasticity has been discussed in many places; an extensive summary with bibliography was given by Bishop *et al.* Rather than dwelling on the details of theory, this paper presents a practical application of hydroelasticity to non-beamlike ships, namely small waterplane area twin-hulled (SWATH) ships. Three SWATH ships or models are involved in this study and they illustrate the strategy of using hydroelasticity as a unified design aid during different stages of design. This includes a case in which detailed structural drawings and mass estimates of the ship were available. As such, this work represents the latest attempt by the authors to understand the difficulties of applying hydroelasticity in assessing the adequacy of designs, particularly those where the latter stages of design have been reached. It is hoped that the material presented will help further establish hydroelasticity as a technique of importance in the study of sea-going vessels.

1. Introduction

The dynamic response behaviour of small waterplane area twin-hull (SWATH) vessels in waves are examined in this paper using a linear, general hydroelasticity theory (Bishop *et al.* 1986), or its modified version (Price & Wu 1989) where fluid viscous damping effects are allowed for in the mathematical model of the theory based on a Morison-type approximation for viscous drag forces. Rather than rehearsing the theory for non-beamlike ships, the purpose of the investigation carried out here is to show the flexibility of applying hydroelasticity as a unified research tool and design aid at different design stages. Three SWATHs are examined with mathematical models of varying degrees of complexity in accordance with design requirements, representing typical applications of the theory at the conceptual, preliminary and detailed design stages respectively.

Unlike hydrodynamic approaches (Lee 1976; Lee & Curphey 1977; McCreight & Stahl 1983; McCreight 1987; Reilly *et al.* 1988), the unified hydroelasticity theory can be used to predict seakeeping performance as well as structural responses of flexible SWATH vessels in waves, without introducing some of the approximations involved in traditional approaches. The assumptions remaining in the hydroelasticity theory include those inherent in the classical potential flow theory and the Morison-type approximation for viscous drag forces. In the results predicted by the hydroelasticity theory the dynamic nature of structural responses of the ship to wave loadings is more thoroughly accounted for.

Phil. Trans. R. Soc. Lond. A (1991) **334**, 339–355
Printed in the Great Britain

The Royal Society is collaborating with JSTOR to digitize, preserve, and extend access to *Philosophical Transactions: Physical Sciences and Engineering.* www.jstor.org

Downloaded from rsta.royalsocietypublishing.org

2. The use of hydroelasticity during the concept design stage

It is important in SWATH design that seakeeping considerations be included at a very early stage without involving structural details and from the viewpoint of hydroelasticity theory, a rigid body model can be adopted at this early stage to estimate approximately the bodily motion responses of the vessel.

In the theory, the generalized equations of motion of a flexible ship in waves take the form

$$(\boldsymbol{a}+\boldsymbol{A})\ddot{\boldsymbol{p}}(t)+(\boldsymbol{b}+\boldsymbol{B})\dot{\boldsymbol{p}}(t)+(\boldsymbol{c}+\boldsymbol{C})\boldsymbol{p}(t)=\boldsymbol{\Xi}\mathrm{e}^{\mathrm{i}\omega_{\mathrm{e}}t}+\boldsymbol{Z}_{\mathrm{d}}(\dot{\boldsymbol{p}},\zeta,\ldots), \tag{1}$$

where $\boldsymbol{a}$, $\boldsymbol{b}$ and $\boldsymbol{c}$ represent, respectively, the $(n\times n)$ generalized mass, generalized structural damping and generalized stiffness matrices of the structure, $\boldsymbol{A}$, $\boldsymbol{B}$ and $\boldsymbol{C}$ represent, respectively, the $(n\times n)$ generalized added mass, generalized hydrodynamic damping and generalized restoring force coefficient matrices of the ship, $\boldsymbol{p}(t)$ denotes the $(n\times 1)$ principal coordinate column matrix, $\boldsymbol{\Xi}(t)$ denotes the $(n\times 1)$ generalized wave excitation column matrix, $\boldsymbol{Z}_{\mathrm{d}}(\dot{\boldsymbol{p}},\zeta,\ldots)$, being generally a nonlinear function of $\dot{\boldsymbol{p}}$, is the $(n\times 1)$ generalized viscous drag force column matrix, ζ is the wave elevation and n is the number of response modes involved in the analysis, the first six modes of which are bodily motion responses.

When a rigid body model is adopted, the principal coordinate vector $\boldsymbol{p}(t)$ in equation (1) is reduced to the (6×1) column matrix

$$\boldsymbol{p}(t)=\{p_1(t),p_2(t),\ldots,p_6(t)\}^{\mathrm{T}}. \tag{2}$$

Here the indices 1, 2, ..., 6 denote surge, sway, heave, roll, pitch and yaw modes respectively. Accordingly, equation (1) is reduced to the traditional equations of motion of hydrodynamics

$$(\boldsymbol{a}+\boldsymbol{A})\ddot{\boldsymbol{p}}(t)+\boldsymbol{B}\dot{\boldsymbol{p}}(t)+\boldsymbol{C}\boldsymbol{p}(t)=\boldsymbol{\Xi}(t)+\boldsymbol{Z}_{\mathrm{d}}(\dot{\boldsymbol{p}},\zeta,\ldots). \tag{3}$$

The information required for the assessment of seaworthiness of the ship includes the global mass properties and a detailed below-water surface geometry description of the ship. A parametric study may be carried out for optimizing the geometrical hull form for a prescribed mission. The coupling effects of distortion modes on bodily motion responses can be assessed at the next design stage when global structural stiffness properties of the ship are specified and wave-induced loads can, thus, be properly estimated.

2.1. SWATH-A

SWATH-A is a scaled model ship (scale factor of 1/20.55). The lower hulls are mainly elliptical in section, with some circular sections towards the aft end. Two pairs of fixed stabilizing fins are fitted. The main particulars of SWATH-A are given in table 1.

2.2. *Hydrodynamic analysis and seakeeping performance of* SWATH-A

The hydrodynamic mesh of SWATH-A adopted in this study is shown in figure 1 and consists of 356-panel elements in a total distributed over the wetted surface of the ship. Using this mesh and a linear, three-dimensional hydroelasticity theory, the interaction between the rigid hull SWATH-A and the surrounding fluid is analysed and the potential flow based generalized hydrodynamic coefficients are derived. The software adopted for the ship–fluid interaction analysis is based on the source distribution method, using the zero-speed Green function together with a forward speed correction (Inglis & Price 1980).

Downloaded from rsta.royalsocietypublishing.org

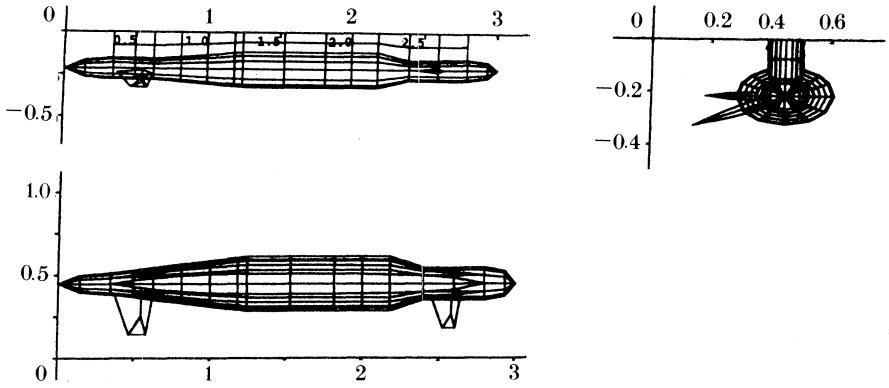

Figure 1. Hydrodynamic mesh of SWATH-A (all lengths in metres).

Table 1. *Main particulars of SWATH-A, SWATH-B and SWATH-C*

item	SWATH-A	SWATH-B	SWATH-C
lower hull length, L/m	3.0049	73.2	70.87
strut length at DWL, LBP/m	2.4554	52.13	57.91
spacing between lower hulls, S/m	0.8939	22.75	21.64
single strut beam on DWL/m	0.1187	2.19	2.74
draught at midship/m	0.3236	8.04	7.54
displacement, ∇/m^3	0.2495	2730.0	3364.0

To predict the seakeeping performance of SWATH-A in waves, viscous drag force effects are included as described by equation (3). The numerical approaches adopted to solve the nonlinear, coupled equations of motion involve Padé approximants in the time domain and a linearization method in the frequency domain (Price & Wu 1989). To estimate the relative motion responses of SWATH-A in regular waves, a particular point at the bow of the model was chosen with the following coordinates in an equilibrium frame system: $x = 1.1926$ m, $y = 0.0$ m, $z = 0.1436$ m. Here the origin of the frame is located at the mean free water surface with the z-axis being vertically upward through the gravity centre of the ship and the Oxy-plane being coincident with the calm water surface.

Figure 2*a*, *b* shows the predicted results for non-dimensional, relative bow motion amplitudes of SWATH-A in regular head waves. Based on Froude number scaling, $Fn = 0.293$, is equivalent to forward speed of 15 knots for the full-scale vessel. In the calculation a constant ratio of wave height over wavelength of $\frac{1}{75}$ was assumed. In these figures the experimental data are denoted by full triangles while the theoretical predictions are denoted by solid lines. As can be seen from this figure a fair correlation is found, on the whole, between the theoretical predictions and model test results except for the case with higher forward speed. Discrepancies may be attributed to the simplification of constant values for C_d and the exclusion of contributions of fins and the lower body to the overall damping due to lift forces. These effects can be included in the mathematical model of the theory without any difficulty by adopting the semi-empirical and experimental results used by McCreight & Stahl (1983).

It must be noted that although the overall structural configuration of a SWATH is non-beamlike, the below-water part of the ship hull is slender, suggesting that fluid

Downloaded from rsta.royalsocietypublishing.org

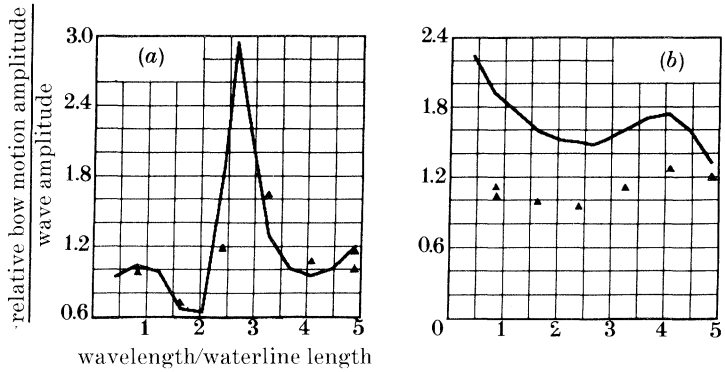

Figure 2. Relative bow motion amplitudes of SWATH-A in regular head waves. (*a*) $Fn = 0$, (*b*) $= 0.293$.

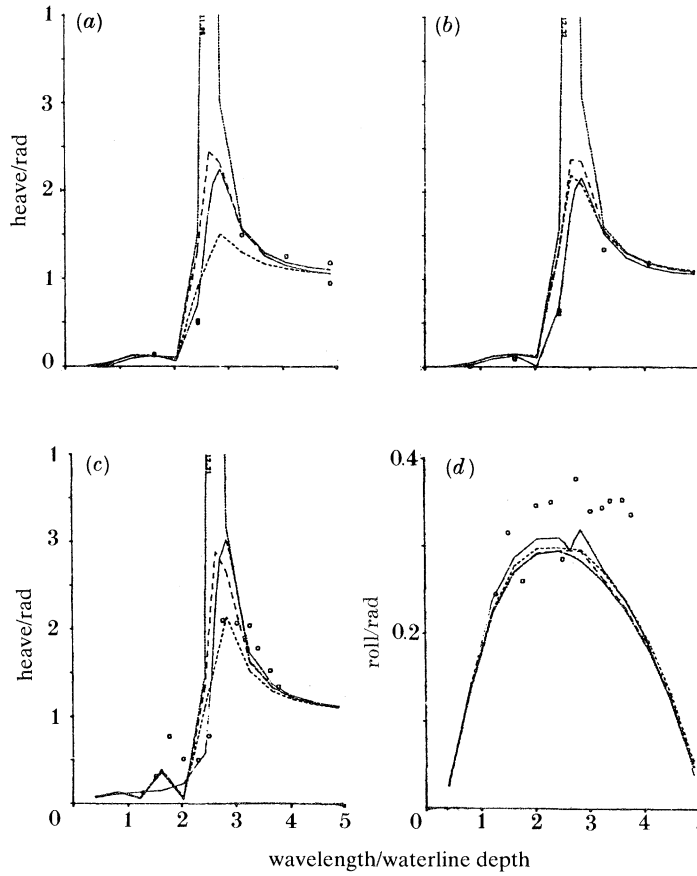

Figure 3. Comparisons between predictions and experimental data for the seakeeping performance of SWATH-A in regular waves. $Fn = 0$. ○, Model; ——, 20; – – –, 30; -------, time; ——, lin. (*a*) Head waves, (*b*) stern waves, (*c*) and (*d*) beam waves.

actions on the lower hulls of the ship might be evaluated approximately on a two-dimensional basis. To confirm this, a two-dimensional hydrodynamic approach (Wu & Price 1987, 1989; Wu 1987) was adopted to predict the seakeeping performance of

Downloaded from rsta.royalsocietypublishing.org

SWATH-A in waves. In this two-dimensional hydrodynamic analysis, a mixed source and dipole distribution method (Wu 1986) is used to obtain wave potential solutions. The forward speed correction is based on the method of Salvesen *et al.* (1970). Following the procedure used by McCreight (1987) viscous drag effects are also accounted for in the two-dimensional analysis. The results are shown in figure 3*a–d* together with the corresponding solutions given by the three-dimensional approach in both the frequency domain and the time domain, and the relevant experimental data of the model tests. In the calculation, a constant wave height of 60 mm was assumed for regular beam waves and a constant ratio of wave height over wavelength of $\frac{1}{75}$ was assumed for regular head and stern waves. These reflect the conditions adopted in the model tests. The corresponding linear, three-dimensional solutions, in which viscous drag force effects are excluded in the analysis, are also given in figure 3 for reference. As can be seen the predictions of the two- and the three-dimensional theories are in good agreement with the experimental data.

3. The use of hydroelasticity at the preliminary design stage

At the preliminary stage of a SWATH design the structural adequacy of the ship is assessed on a global basis. In other words, the main concern of the designers at this stage lies in the estimation of wave-induced primary loads which the main framework of the vessel must withstand.

From a hydroelastic point of view, wave-induced loads in a flexible ship are composed of contributions from individual distortion modes regardless of differences in form and type of ship. Primary wave loads result from global deformation of the ship structure. To determine wave-induced global loads in a flexible SWATH ship, therefore, only a simplified structural model which is constructed on a global, rather than a detailed, equivalence basis is required.

In predicting wave-induced primary loads in a flexible SWATH ship, the seakeeping performance of the vessel is reassessed. In the calculations, the influences of the structural flexibility on bodily motion responses of the vessel are taken into account. The predicted primary wave loads and their distributions throughout the structure provide the important background information for structural design considerations at the detailed design stage.

3.1. *SWATH-B*

SWATH-B is a postulated model proposed originally by Bishop *et al.* (1986). In establishing this model, the published data on SWATH-6A by NSRDC (Lee 1976; Lee & Curphey 1977) were adopted as the basis. The distributions of the global structural stiffness and mass throughout the ship were estimated by rule of thumb. This situation is similar to that occurring at the beginning of the preliminary stage of a SWATH design when structural details of the vessel have not been finalized but the main framework of the structure has been specified. The main particulars of SWATH-B are given in table 1.

3.2. *'Dry' analysis of SWATH-B*

Figure 4*a* illustrates the simplified finite-element idealization adopted for the 'dry' or *in vacuo* analysis of SWATH-B. Quadrilateral facet shell elements which have global in-plane and bending stiffness are used to discretize the box-like cross structure and the struts, while the lower hulls of the vessel are discretized by beam

Downloaded from rsta.royalsocietypublishing.org

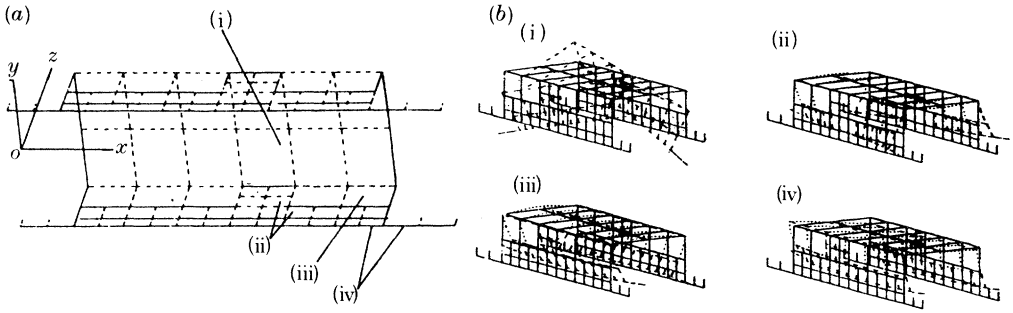

Figure 4. (*a*) The adopted finite-element model and (*b*) the principal mode shapes of the first four distortion modes of SWATH-B *in vacuo*. (*a*) (i) Eight-noded thick facet shell element; (ii) quadrilateral facet shell element; (iii) eight-noded facet shell element; (iv) beam element with offset. (*b*) (i) Mode 7 (A–S), $\omega_7 = 9.52$ rad s^{-1}; (ii) mode 9 (S), $\omega_9 = 12.28$ rad s^{-1}; (iii) mode 8 (S), $\omega_8 = 9.67$ rad s^{-1}; (iv) mode 10 (A–S), $\omega_{10} = 16.72$ rad s^{-1}.

Table 2. *Dynamic characteristics of* SWATH-B

(S, symmetric; AS, antisymmetric.)

modal index, r	mode shape	natural frequency, ω_r rad s^{-1}	generalized mass, a_{rr} kg m$^2 \times 10^6$	generalized stiffness, c_{rr} kg m^2 s$^{-2} \times 10^7$	generalized struc. damping, b_{rr} kg m^2 s$^{-1} \times 10^5$	resonance frequency rad s^{-1}
7	AS	9.52	8.63	7.83	0.85	7.82
8	S	9.67	8.31	7.77	0.87	5.06
9	S	12.28	3.17	4.79	0.43	6.72
10	AS	16.72	1.90	5.30	0.37	10.76
11	S	19.64	0.92	3.56	0.23	11.45
12	AS	19.75	4.58	17.87	1.21	14.73
13	AS	21.45	1.57	7.23	0.47	16.47
14	S	35.26	2.01	25.00	1.13	20.10
15	AS	36.06	2.25	29.24	11.62	21.81
16	S	58.37	2.68	9.13	0.59	48.75

elements with offset, which have axial, torsional and bending stiffness. This simplified, but globally equivalent, finite-element model of SWATH-B consists of 32 beam elements, 42 thin quadrilateral facet shell elements for the two struts and 12 thick quadrilateral facet shell elements for the cross structure. In total, there are 86 elements, 163 nodes and approximately 750 degrees of freedom.

The 'dry' analysis of SWATH-B was performed using PAFEC. The first four distortion modes derived from the undamped free vibration analysis of SWATH-B are shown in figure 4*b*. These distortion modes divide themselves into two distinct groups, i.e. modes $r = 8, 9$ are symmetric with respect to the vertical centreline-plane, and modes $r = 7, 10$ are antisymmetric. As can be seen from figure 4*b* none of these modes can be regarded as a local distortion mode. The modal characteristics of the first ten distortion modes of SWATH-B are given in table 2 including the assumed generalized structural damping coefficients.

Downloaded from rsta.royalsocietypublishing.org

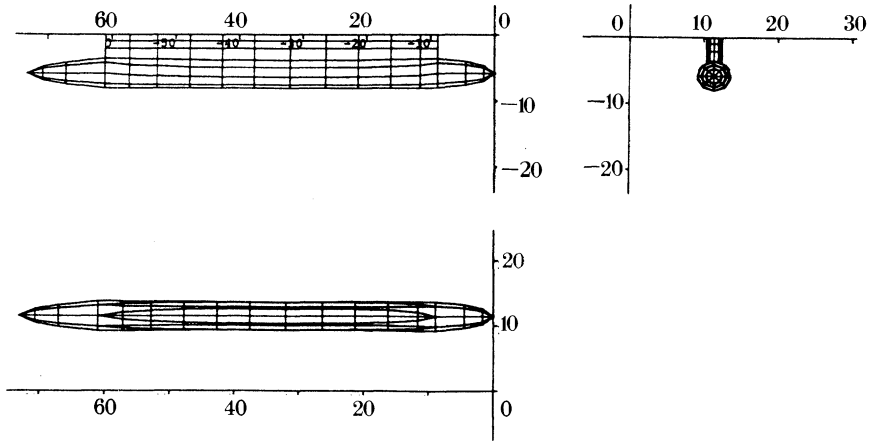

Figure 5. Hydrodynamic mesh of SWATH-B (all lengths in metres).

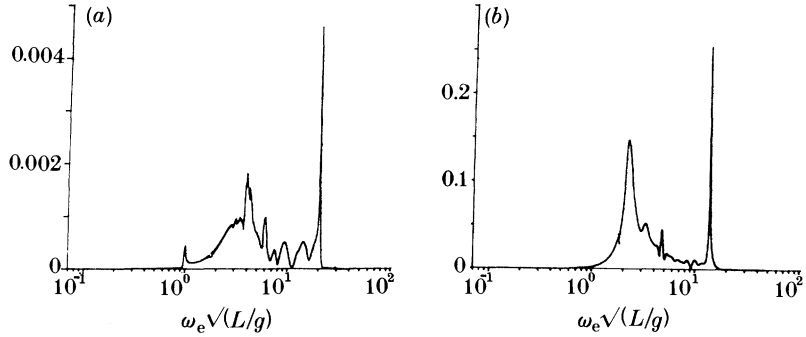

Figure 6. Principal coordinate amplitudes (*a*) $|p_7|$ and (*b*) $|p_8|$ of SWATH-B in regular beam waves of unit amplitude. ——, Vis. included; – – – –, vis. excluded.

3.3. *'Wet' analysis of SWATH-B*

Figure 5 shows the hydrodynamic mesh adopted in the 'wet' analysis of SWATH-B. The mean wetted surface of the ship is discretized by 432 panel elements, 28 of which are used for the two pairs of the stabilizing fins (not shown in the figure). In the study, the SWATH is assumed to travel in waves at 11.6 knots ($Fn = 0.223$). The 'wet' analysis was performed using the linear hydroelasticity theory. It produces corresponding generalized hydrodynamic coefficients and the generalized wave excitation. Combining the results from the 'dry' analysis and the 'wet' analysis and including the nonlinear viscous drag force effects allow the corresponding principal coordinates to be determined. In the calculations a linearization method in the frequency domain was used. These results are not illustrated here as they can be found elsewhere (Bishop *et al.* 1986; Price *et al.* 1987*a*, *b*).

The 'wet' resonance frequencies for the first ten distortion modes are also given in table 2 showing the overall hydrodynamic effects on the dynamic characteristics of SWATH-B in waves. Different values for the ratio of 'wet' resonance frequency over 'dry' natural frequency can be seen, e.g. 0.82 for mode $r = 7$, 0.52 for mode $r = 8$, etc. The amplitudes of principal coordinates corresponding to modes $r = 7$ and 8 are shown in figure 6 for SWATH-B travelling at 11.6 knots in regular beam waves of unit amplitude ($a = 1$ m).

Downloaded from rsta.royalsocietypublishing.org

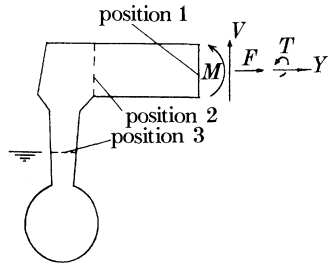

Figure 7. Schematic representation of primary wave-induced loads and positions of interest on SWATH-B. M, Transverse bending moment; T, torsion moment; F, in-plane force; V, shearing force.

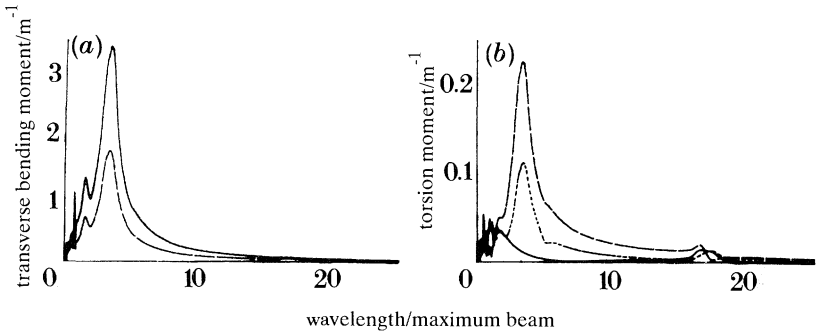

Figure 8. The non-dimensional (a) transverse bending and (b) torsional moment amplitudes at different positions of SWATH-B in regular beam waves of unit amplitude. ——, Position 1; – – – –, position 2; — — —, position 3.

3.4. *Primary wave loads at different locations of SWATH-B*

Transverse strength is of particular importance in structural design of SWATHs. Within the ship structure three longitudinal sections are of special interest to designers at this stage. These are the middle section of the cross structure, which is equivalent to the amidship section of a conventional monohull ship, and the two junction sections between the three structural components, namely, the submerged lower hulls, the water surface piercing struts and the above-water cross structure, where the structural configuration of the ship has a substantial change. These three typical locations are designated as position 1, position 2 and position 3 respectively and are shown in figure 7 together with the primary wave loads concerned.

A selection of the derived primary wave loads of SWATH-B travelling at 11.6 knots in regular beam waves is shown in figure 8a, b. These wave loads are non-dimensionalized as stated in table 3. Figure 8a shows the predicted non-dimensional transverse bending moment responses at different locations in SWATH-B. The results clearly suggest that the peak bending moment at position 1 is the greatest and is approximately double of the peak value at position 3. The roll resonance occurring at $\lambda/B_0 = 17.5$ has no effect on the bending moment responses at position 1 and very small effect at positions 2 and 3. Figure 8b shows the predicted non-dimensional torsional moment response amplitudes at different locations of SWATH-B. It is clearly seen from the figure that the greatest peak value occurs at position 3 in this wave heading. At long wavelengths ($\lambda/B_0 \geqslant 5.0$) there is almost no torsional moment acting at position 1 of the ship. Table 3 summarizes the critical primary wave loads at the three positions of SWATH-B deduced from the investigation (Price *et al.* 1987b).

Downloaded from rsta.royalsocietypublishing.org

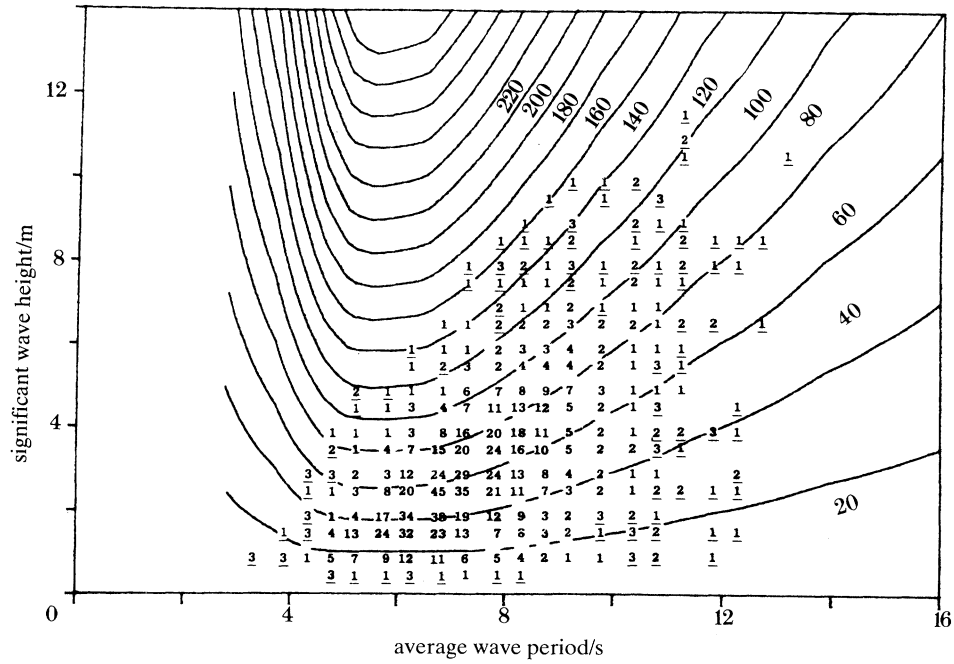

Figure 9. Contours of the significant transverse bending moment at position 1 of SWATH-B when travelling at 11.6 knots in unidirectional irregular beam seas (described by ISSC wave spectra) together with recorded wave data (Fortnum 1978). Values of $|M_{\mathrm{tr}}|_{\frac{1}{3}}$ in meganewton metres are given towards the right-hand end of the curves.

Table 3. *Critical non-dimensional wave loads at critical positions of SWATH-B travelling at 11.6 knots in regular seaways of unit wave amplitude*

(The forces and moments are non-dimensionalized by $(\rho\nabla a/\mathrm{L})$ and $(\rho\nabla a)$, respectively, where ρ = density of water, a = wave amplitude and B_0 is the maximum beam of the vessel.)

wave load	heading	position	λ/B_0	response
transverse bending moment	beam waves	1 and 2	3.3	3.4
	beam waves	3	3.3	1.8
torsional moment	beam waves	3	3.3	0.23
	bow waves	1	2.5	0.21
	beam waves	2	3.3	0.12
in-plane force	beam waves	1 and 2	3.3	20.0
vertical shear force	beam waves	2	3.3	10.0

Experimental data available for various SWATH models (see, for example, Lee & Curphey 1977; Sikora 1988; Reilly *et al.* 1988) confirm the predictions given in table 3.

3.5. *SWATH-B in irregular seas: application to design*

The predicted statistical properties of the primary wave loads on SWATH-B in irregular seas can be combined with appropriate wave data to produce important information for design consideration (Price *et al.* 1987*a*, *b*).

The extreme value of wave loads derived from the combination of the predictions of loads with wave statistics may be visualized as shown in figure 9, for the significant transverse bending moment at position 1 of the ship. In these calculations, the two-

Downloaded from rsta.royalsocietypublishing.org

parameter ISSC wave spectrum was used. In this figure, the contour map of the significant bending moment is superimposed with wave data recorded in the northern North Sea (Fortnum 1978) during the winters between the years 1969 and 1976. The plain numbers in the figure indicate per thousand exceedances while the underlined numbers indicate the number of occurrences for the whole of the duration of the measurements. The extreme value of the significant transverse bending moment at position 1 of the ship under such sea conditions is about 170 MN m.

4. The use of hydroelasticity at the final design stage

At the final stage of a SWATH design the structural adequacy of the ship is assessed on a detailed basis. In other words, the main concern of designers at this stage lies in the prediction of stress responses in the ship for given loading conditions. This necessitates the use of a detailed structural model.

Traditionally, a static or quasi-static analytical method is used to calculate dynamic stress responses of a SWATH in waves. This involves determination of hydrodynamic pressure distributions along the hulls from a seakeeping theory and, consequently, the introduction of simplified force boundary conditions. A typical example of applying this traditional approach to a case study on the SWATH T-AGOS 19 design was given by Reilly *et al.* (1988). In assessing the structural adequacy of the SWATH, structural analyses of the ship were performed as many times as required by the prescribed wave loading conditions.

From a hydroelastic point of view, stress responses in a flexible SWATH structure are composed of contributions from global and local distortion modes. Primary stress responses result from global deformation of the structure. If only predictions of primary stress responses in the ship are of interest, it follows that local distortion modes need not be included in the mathematical model. Using a hydroelastic approach, a 'dry' analysis of the detailed model is performed only once to determine the modal characteristics of the structure *in vacuo* so that the whole structure–fluid system can be transformed into a new one described in a modal space with a reduced number of degrees of freedom. The subsequent calculation involves the determination of generalized hydrodynamic coefficients, wave excitations and viscous drag forces of the SWATH for a given sea condition. These combined with the generalized structural properties of the ship allow the principal coordinates to be determined as for equation (1). Stress responses in the SWATH are obtained by modal summations involving the modal stress fields and the corresponding principal coordinates. Meanwhile, the seaworthiness of the SWATH is once again reassessed.

4.1. *SWATH-C*

SWATH-C is based on the T-AGOS 19 SWATH (see Reilly *et al.* 1988). The main particulars of the vessel are given in table 1.

4.2. *'Dry' analysis of SWATH-C*

The finite-element model adopted in this study takes account of the entire vessel by modelling all the principal steel-work and stiffeners using plate, shell and beam elements with remaining items, including those not contributing to the structure, represented by beams or point and distributed masses. Since stresses in the SWATH due to local distortion modes are not considered here and no particular areas within the structure are of special interest, some simplifications were introduced in

PHILOSOPHICAL TRANSACTIONS OF THE ROYAL SOCIETY A MATHEMATICAL, PHYSICAL & ENGINEERING SCIENCES

PHILOSOPHICAL TRANSACTIONS OF THE ROYAL SOCIETY A MATHEMATICAL, PHYSICAL & ENGINEERING SCIENCES

Downloaded from rsta.royalsocietypublishing.org

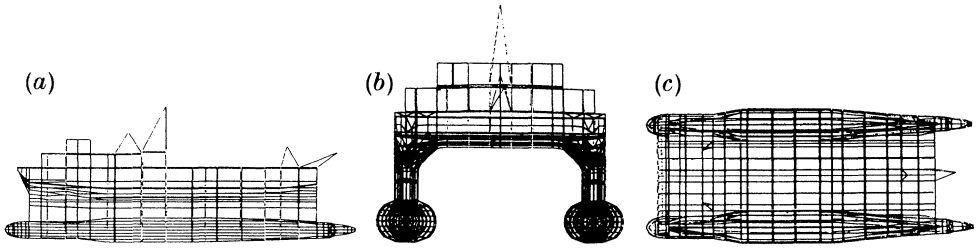

Figure 10. (*a*) Side, (*b*) front and (*c*) top views of the finite element model for SWATH-C.

modelling local structural details, such as accounting for small openings in transverse bulkheads by systematic reduction in the thickness of the plate elements modelling the bulkheads, use of equivalent thickness for stiffened plating, etc.

A mixture of semi-loof curved plate elements, flat shell elements and simple beam elements were used to discretize the SWATH-C structure. For simplicity the structure (but not the masses used to model equipments and so on) were taken to be exactly symmetric about the vertical centreline plane. Triangular elements have only been adopted where rapid changes of structural shape make the use of quadrilateral elements impossible or in transition areas where the mesh density changes. In all, the detailed finite-element model adopted consists of approximately 4700 elements with 34000 degrees of freedom, of which 343 elements are discrete masses and 393 beams. Figure 10 shows various views of the finite-element idealization of SWATH-C adopted in this study.

The 'dry' analysis of SWATH-C was performed once again using the PAFEC finite element software. The selected number of master degrees of freedom is 200 with the results of the first third of the calculated modes being reliable. Of the 200 calculated modes the first 48 are rigid modes (i.e. six true rigid body modes and 42 due to lumped masses being attached to isoparametric elements with no associated stiffnesses to model a number of large items of equipment on the vessel).

Among the next 50 (non-rigid body) modes, 35 are identified as being localized with only two being very clearly global (i.e. mode 51 and mode 59 in table 4). Of the remaining thirteen, the eight with the most obvious below-water distortion are selected for inclusion within the 'wet' analysis, giving ten distortion modes in total to be used for the prediction of primary stress responses in the vessel. These ten modes are listed in table 4.

To gain an understanding of the effect of combined primary stresses in the SWATH structure, the von Mises stress can be calculated as an effective stress and this may be related to the condition of yielding of the material used. The von Mises stress, σ_e, is defined in terms of the direct and shear stresses by

$$\sigma_e = \sqrt{\{\tfrac{1}{2}[(\sigma_x-\sigma_y)^2+(\sigma_y-\sigma_z)^2+(\sigma_x-\sigma_x)^2]+3(\tau_{xy}^2+\tau_{yz}^2+\tau_{zx}^2)\}}, \tag{4}$$

where, for example, $\sigma_x \equiv \sigma_x(x, y, z, t)$.

In fact, the von Mises stress represents, except for a constant factor, the potential energy of distortion stored in the material under pure elastic strains (Nadai 1931). Examples of the modal von Mises stress fields derived for modes 51 and 59 are illustrated in figure 11*a*, *b*, plate 1. As expected these figures reveal high stresses in the regions where localized, large-amplitude distortions occur. Examination of the ten principal model deflections, which are not illustrated here, shows that the stern ends of the lower hulls are highly flexible, while the cross structure seems quite rigid.

Downloaded from rsta.royalsocietypublishing.org

Table 4. *The global distortion modes of* SWATH-C
(Numbers in brackets indicate the mode index number.)

modal number	natural freq. Hz	generalized mass/t	modal number	natural freq. Hz	generalized mass/t
51 ($r = 7$)	0.894	722.0	85 ($r = 12$)	2.984	0.707
59 ($r = 8$)	1.799	81.5	87 ($r = 13$)	2.991	2.96
63 ($r = 9$)	1.844	2.27	88 ($r = 14$)	2.993	1.40
78 ($r = 10$)	2.780	3.72	94 ($r = 15$)	3.099	1.83
79 ($r = 11$)	2.848	2.40	97 ($r = 16$)	2.130	0.828

4.3. *'Wet' analysis of* SWATH-C

For convenience a one-to-one correspondence between the finite element mesh on the wetted surface of the hull and the panel discretizations was adopted, thus providing a hydrodynamic mesh consisting of 573 panels for the port half of the SWATH.

In the calculation, the potential flow based, generalized hydrodynamic coefficients and wave excitations have been evaluated for frequencies between 0.02 and 3.34 Hz, covering the entire frequency range of the selected ten distortion modes. Effort was concentrated in a low wave frequency range ($\omega_e < 0.5$ Hz) where significant variations of the hydrodynamic coefficients are expected and where the dominant wave frequencies in a seaway occur.

Figure 12*a*, *b* illustrate the calculated principal coordinate amplitudes of SWATH-C travelling at 3.0 knots in regular beam waves of unit amplitude for the first two global distortion modes. By comparison with the principal coordinate amplitudes for SWATH-B travelling at 11.6 knots in regular beam waves of unit amplitude as shown in figure 6*a*, *b* it can be seen that these two principal coordinate amplitude curves, namely, $|p_7|$, $|p_8|$, are very similar throughout the frequency range shown, strongly suggesting that mode 51 of SWATH-C corresponds to mode 7 of SWATH-B, while mode 59 of SWATH-C corresponds to mode 8 of SWATH-B; in other words, mode 51 and mode 59 of SWATH-C are the two fundamental global distortion modes of the vessel, the former being antisymmetric and the latter being symmetric. Investigation of the remaining principal coordinates reveals that they are likely to be predominantly local distortion modes rather than global ones.

4.4. *Primary stresses of* SWATH-C *in irregular seas*

When the seaways of interest are described by the two parameter ISSC wave spectrum, the root mean square (r.m.s.) value of the von Mises stress responses at a point (x, y, z) within the structure is then given by

$$[\sigma_e(x, y, z)]_{\text{r.m.s.}} = \sqrt{\left(\int_0^\infty |\text{RAO}_{\sigma_e}|^2 \Phi_{\zeta\zeta}(\omega_e)\, \mathrm{d}\omega_e \right)}, \tag{5}$$

where RAO_{σ_e} denotes the response amplitude operator of the von Mises stress at point (x, y, z) and $\Phi_{\zeta\zeta}$ is the wave spectrum used.

To allow a simple numerical comparison between the results of the predicted primary stress response in the SWATH structure under different wave loading conditions, an average process over the estimated von Mises stresses at all points of the structure was taken to produce a single value for each condition. The derived results can best be interpreted in the form of a polar plot indicating how heading angle,

PHILOSOPHICAL TRANSACTIONS OF THE ROYAL SOCIETY A MATHEMATICAL, PHYSICAL & ENGINEERING SCIENCES
PHILOSOPHICAL TRANSACTIONS OF THE ROYAL SOCIETY A MATHEMATICAL, PHYSICAL & ENGINEERING SCIENCES

Downloaded from rsta.royalsocietypublishing.org

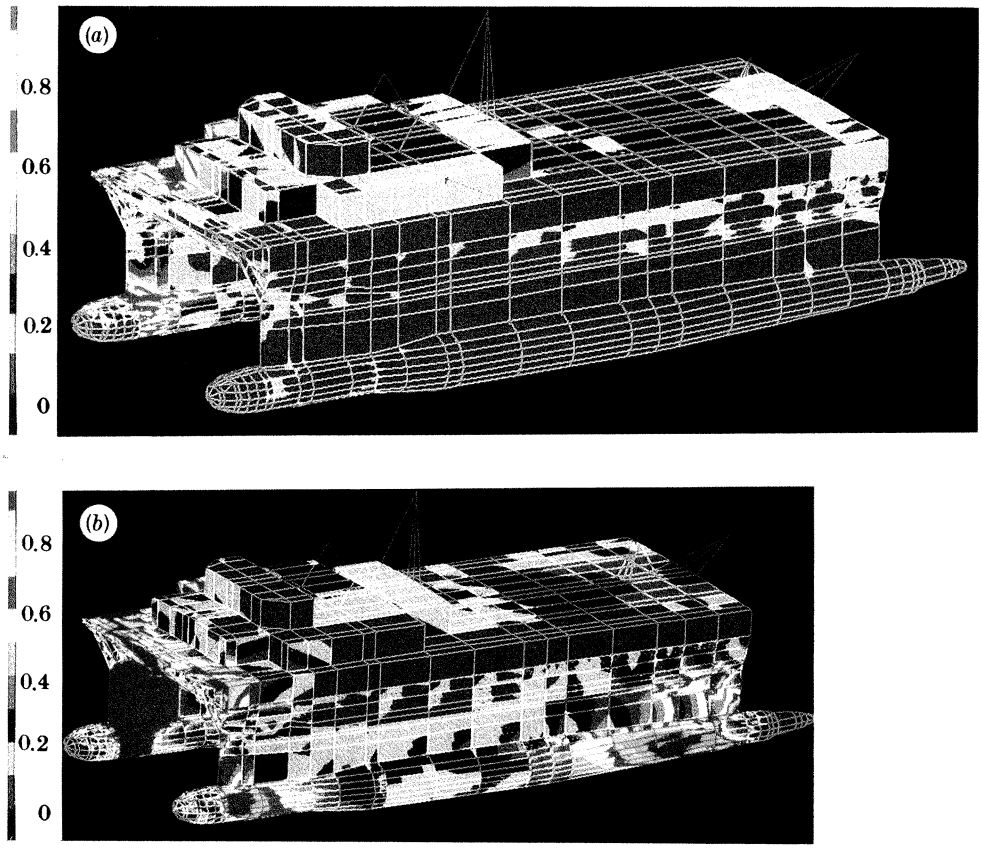

Figure 11. Three-dimensional contour pictures of the finite-element model showing the von Mises stress fields on SWATH-C for (*a*) mode 51 ($r = 7$) and (*b*) mode 59 ($r = 8$). Stress levels in megapascals.

PHILOSOPHICAL TRANSACTIONS OF THE ROYAL SOCIETY A MATHEMATICAL, PHYSICAL & ENGINEERING SCIENCES

PHILOSOPHICAL TRANSACTIONS OF THE ROYAL SOCIETY A MATHEMATICAL, PHYSICAL & ENGINEERING SCIENCES

Downloaded from rsta.royalsocietypublishing.org

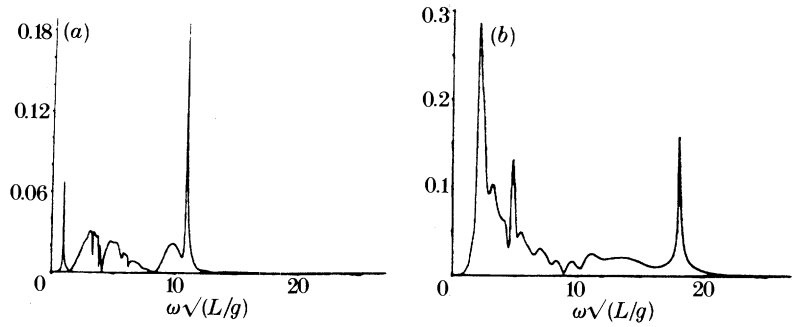

Figure 12. Principal coordinate amplitudes (*a*) $|p_7|$ and (*b*) $|p_8|$ of SWATH-C in regular beam waves of unit amplitude. (*a*) Mode 51; (*b*) mode 59.

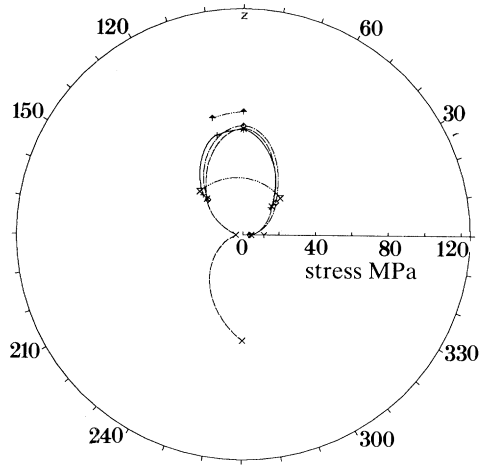

Figure 13. Variation of the spatial mean r.m.s. von Mises stress with speed, heading and sea state (180° corresponds to hard seas). ——, 0 knots, S/S 6; – – – –, 3 knots, S/S 6; —– —–, 8 knots, S/S 6; —– —–, 0 knots, S/S 7; — — — — — — —, 3 knots, S/S 7; , 0 knots, S/S 9; , 3 knots, S/S 9.

speed and sea-state affect the stress response levels of the structure as shown in figure 13. As can be seen from this figure the higher sea states tend to increase the stress response levels for a given direction and speed, with beam seas giving the most extreme case.

If one examines the spatial distributions of the r.m.s. von Mises stress, the following comments on stress levels can be made.

1. The lower hulls at the strut aft ends are highly stressed. This is presumably due to the rather narrow transverse bulkheads in this region that must support the considerable overhang of the lower hulls with heavy propellers attached at their extreme ends.

2. The lower hulls at the strut forward ends are significantly stressed, again presumably due to the combination of overhang and narrow transverse bulkheads. These stresses are not so severe as those at the aft ends of the lower hulls.

3. The cross structure outboard of the longitudinal bulkheads are lightly stressed even in the most extreme load case.

4. The main deck between the two longitudinal bulkheads is stressed more highly than the surrounding structure, particular at the aft end.

Downloaded from rsta.royalsocietypublishing.org

5. The superstructure cannot be regarded as structurally ineffective. Stress levels in the superstructure particularly near the forward outer edges are of the same order as large areas of the struts and the main deck.

5. Conclusions

The main conclusions from this investigation are summarized below.

1. The significant advantage of the hydroelastic approach over the traditional hydrodynamic methods in describing the overall dynamics of a non-beamlike flexible structure, such as a SWATH, is that dynamic structural responses (i.e. distortions, bending moments, torsional moments, stresses, etc.) of the flexible ship in waves are estimated by the theory directly from first principles without invoking previous experience or additional assumptions. This is particularly important to designers when the structure under consideration is completely or partly new and no database of successful designs of any kind can be relied on.

2. The mathematical model adopted in a hydroelastic analysis of a ship can be constructed with varying degrees of complexity in line with the requirements at different design stages. That is, regardless of differences in form and type of ships, a rigid body mathematical model *can* be adopted at the concept design stage to estimate approximately the seakeeping performance of the vessel; a simplified finite-element model can be used at the preliminary design stage to predict the primary wave loads exerted on the main framework of the structure and to re-check the seaworthiness of the vessel when the influence of structural flexibility on bodily motion responses are included; a detailed finite-element model can be used at the final design stage to assess the structural adequacy of the design according to the predicted dynamic stress levels within the structure and once again to re-check the seaworthiness of the vessel.

3. Apart from the potential flow based fluid forces, if required, other sources of dynamic fluid actions on structures can be readily included in the three-dimensional hydroelasticity theory without modifying the general approach.

4. Non-beamlike ships are characterized by three-dimensional form of the structure and therefore the simple beam theory of structural dynamics is no longer adequate to describe the overall dynamics of the ships. In some cases, fluid actions on non-beamlike ships (like a SWATH) may be approximately described on a two-dimensional basis (Lee 1976; Lee & Curphey 1977), while in other cases, fluid actions on non-beamlike ships are featured by three-dimensional effects (Lundgren *et al.* 1989). A hybrid, three-dimensional structure and two-dimensional fluid analysis may be thought of more practical use in design process in particular for SWATH vessels. In all cases, the general three-dimensional hydroelasticity theory can be applied to predict wave-induced motions, global loads and especially dynamic stresses on any vessels in a seaway.

5. Resonance behaviour of vessels in waves can be clearly predicted by hydroelasticity theory as demonstrated in this study. In general, exclusion of structural flexibility effects would result in an overestimation of wave-induced loads in the vessel in the low wave frequency region and would lead to an underestimation of the statistical structural responses of the vessel in realistic seaways, in which the random nature of the sea environment and resonance effects have to be taken into account.

PHILOSOPHICAL TRANSACTIONS OF THE ROYAL SOCIETY A MATHEMATICAL, PHYSICAL & ENGINEERING SCIENCES

PHILOSOPHICAL TRANSACTIONS OF THE ROYAL SOCIETY A MATHEMATICAL, PHYSICAL & ENGINEERING SCIENCES

Downloaded from rsta.royalsocietypublishing.org

References

Bishop, R. E. D. & Price, W. G. 1979 *Hydroelasticity of ships*. Cambridge University Press.

Bishop, R. E. D., Price, W. G. & Temarel, P. 1986 On the hydroelastic response of a SWATH to regular oblique waves. In *Advances in marine structures* (ed. C. Smith & J. Clarke), pp. 89–110. London: Elsevier.

Bishop, R. E. D., Price, W. G. & Wu, Yousheng 1986 A general linear hydroelasticity of floating structure moving in a seaway. *Phil. Trans. R. Soc. Lond.* A **316**, 375–426.

Fortnum, B. C. H. 1978 Waves recorded by MV Famita in the northern North Sea: data for winters of 1969 to 1976 at 57° 30′ *N*, 01° 00′ *S*. *Inst. Oceanographic Sci. Rep.* no. 69.

Inglis, R. B. & Price, W. G. 1980 Comparison of calculated responses for arbitrary shaped bodies using two- and three-dimensional theories. *Int. Shipbuilding Prog.* **27**, 86–95.

Lee, C. M. 1976 Theoretical prediction of motion of small waterplane area twin hull (SWATH) ships in waves. *DTNSRDC Rep.* SPD-76-0046.

Lee, C. M. & Curphey, R. M. 1977 Prediction of motion, stability and wave load of small waterplane twin hull ships. *Trans. SNAME* **85**, 94–130.

Lundgren, J., Price, W. G. & Wu, Yongshu 1989 A hydroelastic investigation into the behaviour of a floating 'dry' dock in waves. *Trans. RINA* **131**, 213–231.

McCreight, K. K. 1987 Assessing the seaworthiness of SWATH ships. *Trans. SNAME* **95**, 189–214.

McCreight, K. K. & Stahl, R. 1983 Vertical plane motions of SWATH ships in regular waves. *DTNSRDC Rep.* SPD-1076-01.

Nadai, A. 1931 *Plasticity*. McGraw-Hill.

Price, W. G. & Bishop, R. E. D. 1974 *Probabilistic theory of ship dynamics*. London: Chapman and Hall.

Price, W. G., Temarel, P. & Wu, Yongshu 1987*a* Wave loads experienced by SWATHs in waves. Int. Symp. on Advanced Research for Ships and Shipping in the Nineties, Genoa, Italy.

Price, W. G., Temarel, P. & Wu, Yongshu, 1987*b* Responses of a SWATH travelling in irregular seas. *J. Underwater Technol., U.K.* **13**, 2–10.

Price, W. G. & Wu, Yongshu 1989 The influence of non-linear fluid forces in the time domain responses of flexible SWATH ships excited by a seaway. OMAE 89, vol. 2, pp. 125–135, Hague, The Netherlands.

Reilly, E. T., Shin, Y. S. & Kotte, E. H. 1988 A prediction of structural load and response of a SWATH ship in waves. *J. nav. Engrs* 251–264.

Salvesen, N., Tuck, E. O. & Faltinsen, O. 1970 Ship motion and sea loads. *SNAME Annual Meeting*, Pap. no. 6, New York.

Sikora, J. P. 1988 Some design approaches for reducing the structural weight of SWATH ship. Int. Conf. on SWATH Ships and Advanced Multi-Hulled Vessels II, vol. 2, RINA, paper no. 18, London.

Wu, X.-J. 1986 A two-dimensional source-dipole method for seakeeping analysis of ships and offshore structures. CADMO 86, pp. 223–235, Springer-Verlag.

Wu, X.-J. 1987 SWATH ship motion and wave loading analysis program: WUSWATH. Report, Dept Mech. Eng., Brunel University.

Wu, X.-J. & Price, W. G. 1987 A multiple Green's function expression for the hydrodynamic analysis of multi-hull structures. *Appl. Ocean Res.* **9**, 58–66.

Wu, X.-J. & Price, W. G. 1989 Solution approximations to the horizontal plane motions of full-bodied slender or shallow draft marine structures. *Int. Shipbuilding Prog.* **36**, 237–282.

Discussion

D. W. CHALMERS (*HMS Saker, BFPO 2, U.K.*). Dr Smith (this symposium) shows that linear strip theory significantly overestimates structural responses compared with measurements from sea. Is there any evidence that SWATH responses are similarly overestimated or are the numerical predictions better? It appears that they

PHILOSOPHICAL TRANSACTIONS OF THE ROYAL SOCIETY A MATHEMATICAL, PHYSICAL & ENGINEERING SCIENCES

PHILOSOPHICAL TRANSACTIONS OF THE ROYAL SOCIETY A MATHEMATICAL, PHYSICAL & ENGINEERING SCIENCES

Downloaded from rsta.royalsocietypublishing.org

could be so as the structure is more nearly wall-sided and symmetrical about the still waterline than a conventional monohull vessel.

A. J. Keane. Experimental data for structural responses are not available to us for either SWATH-B or SWATH-C. It is, therefore, difficult to provide Dr Chalmers with a straightforward answer except to say it seems likely (Lundgren *et al.* 1989).

K. Nicholson (*Portsdown, U.K.*). An early slide showed the relatively narrow response peaks for all the rigid body motions compared with those for a monohull, with the possible exception of roll. The figure suggests the possibility of using active motion control to reduce these responses. Does Dr Keane incorporate active control, and the associated forces on the structure, in his subsequent analysis, and if so, what difference it made?

A. J. Keane. Our present results do not incorporate active control although SWATHs, in general, have active fin controllers. Our interest mainly lies in establishing the motion characteristics of such vessels and the parameters which affect them rather than assessing the means of enhancing these characteristics.

A. Incecik (*University of Glasgow, U.K.*). Since the structural response of free-floating twin hull structures could be sensitive to boundary conditions, mass distribution, and hydrodynamic damping, did Dr Keane quantify the importance of such conditions and parameters in the structural response predictions?

When a free-floating twin-hull structure is analysed in a beam sea condition using a quasi-static analysis technique, maximum bending moment occurs at the centre of the deck when the wavelength is equal to twice the spacing between the hulls. When the three-dimensional hydrodynamic loading program is used and the structure is analysed under dynamic loading, can Dr Keane define a ratio between the wavelength and hull spacing at which maximum bending moment at the centre of the deck occurs? Can he also illustrate comparisons between the structural response predictions obtained from their dynamic analysis with those obtained from a quasi-static analysis?

A. J. Keane. Variables, such as mass distribution and hydrodynamic damping, referred to by Dr Incecik, affect the structural responses of monohulls as well as twin hulls. They are implicit in a hydroelastic analysis, i.e. in the construction of an appropriate structural model and also in the subsequent fluid–structure interaction analysis. However, considering the effort involved in carrying out a complete analysis, we have only produced results for nominal load conditions. Regarding transverse bending moment responses at the centre of the cross deck of a SWATH in regular beam waves, we have observed similar qualitative trends in the predictions given by both the hydroelastic, and the quasi-static analysis methods. For example, in our study the predicted maximum bending moment of SWATH-B occurs at a wavelength 3.3 times the maximum overall beam of the ship as given in table 3 of the paper, while Lee & Curphey (1977) predicted the large peak of the bending moment occurring at wavelengths roughly three to four times the maximum overall beam of SWATHs using a quasi-static method.

S. Hylarides (*Wageningen, The Netherlands*). In the calculation of the forced, global

PHILOSOPHICAL TRANSACTIONS OF THE ROYAL SOCIETY A MATHEMATICAL, PHYSICAL & ENGINEERING SCIENCES

Downloaded from rsta.royalsocietypublishing.org

response Dr Keane has used ten vibration modes with fixed damping factors, as shown on one of the slides. It seems that these damping factors are rather high. Moreover, they increase gradually with the mode number, running from about 5% to 12% of the critical damping. This can only be structural damping, whereas in the considered frequency range the hydrodynamic damping is practically zero. Why should the damping take these values, especially accounting for the fact that they were dealing with a completely new ship type for which no information at all is available? Already for conventional ship types the selection of damping for the lower hull modes is rather arbitrary, only an order of magnitude can be indicated.

A. J. Keane. Professor Hylarides's comments reveal an area where information – experimental or otherwise – is hard to come by, namely the structural damping levels. These, consequently, were chosen arbitrarily. Such a choice, however, will only have a quantitative influence on the structural responses in the immediate vicinity of the resonances.

W. Beukelman (*Delft University of Technology, The Netherlands*). I was impressed by Dr Keane's presentation related to the determination of the load on SWATH ships. As I understood it, slamming pressures are not taken into account. These pressures may be very high for these ships as reported by Mr N. Pegg at the IUTAM Conference, especially at the forward part and at high speed in a seaway. Should these pressures be accounted for in the future?

A. J. Keane. Professor Beukelman draws our attention to the effects of slamming, in particular the slamming induced pressures at the forward part of the bridge structure, on the structural responses of a SWATH. We are actively engaged in providing the means for incorporating such loads into the hydroelasticity analysis.

Colour plate printed in Great Britain by George Over Limited, London and Rugby.

PHILOSOPHICAL TRANSACTIONS OF THE ROYAL SOCIETY A MATHEMATICAL, PHYSICAL & ENGINEERING SCIENCES

PHILOSOPHICAL TRANSACTIONS OF THE ROYAL SOCIETY A MATHEMATICAL, PHYSICAL & ENGINEERING SCIENCES

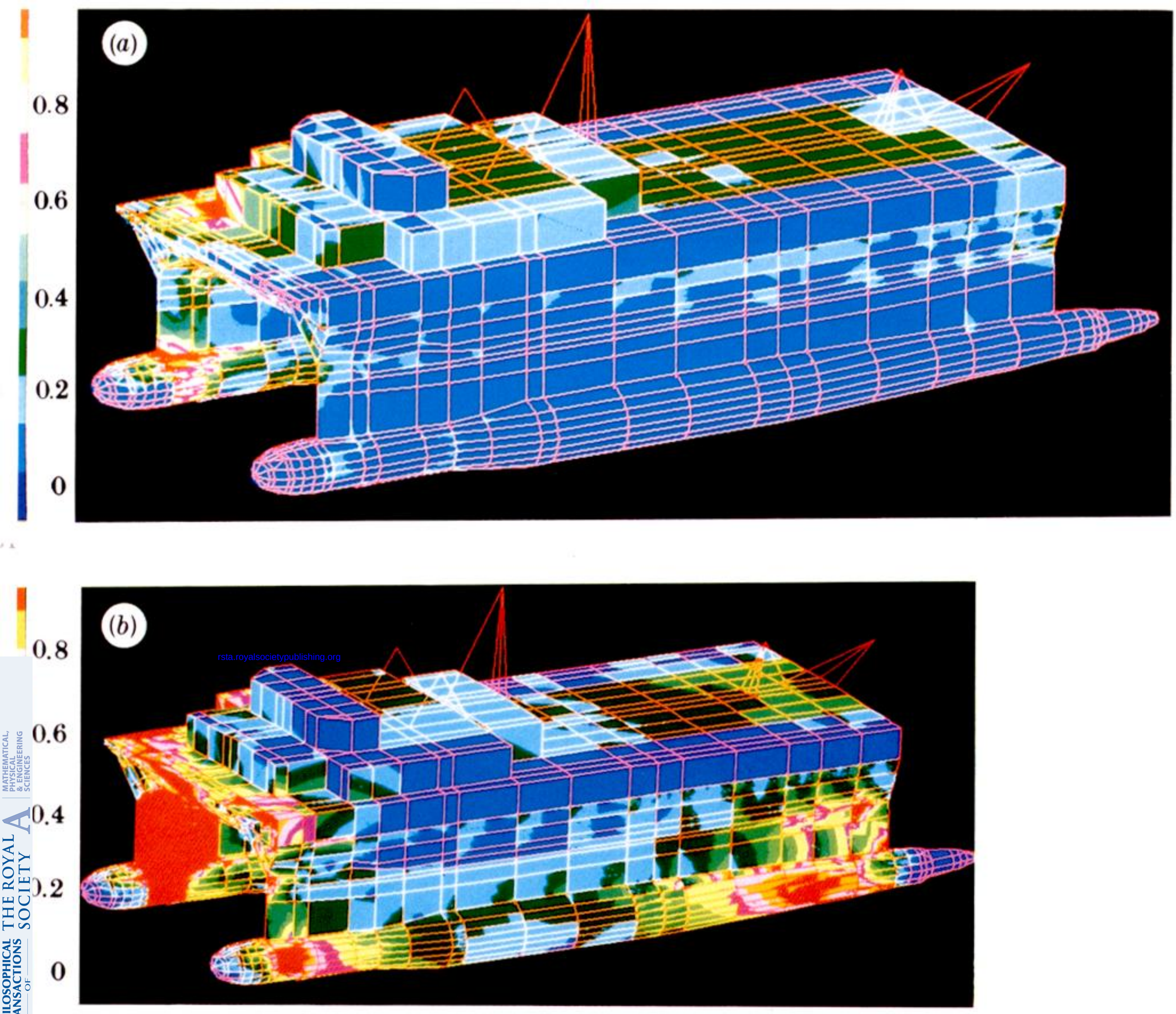

rsta.royalsocietypublishing.org

PHILOSOPHICAL TRANSACTIONS OF THE ROYAL SOCIETY A MATHEMATICAL, PHYSICAL & ENGINEERING SCIENCES

PHILOSOPHICAL TRANSACTIONS OF THE ROYAL SOCIETY A MATHEMATICAL, PHYSICAL & ENGINEERING SCIENCES

igure 11. Three-dimensional contour pictures of the finite-element model showing the von lises stress fields on SWATH-C for (*a*) mode 51 ($r = 7$) and (*b*) mode 59 ($r = 8$). Stress levels in egapascals.